60 GHz square open-loop resonator (SOLR) based on planar Goubau line (PGL) technology

Emad Elrifai, Marjorie Grzeskowiak, Gaelle Bazin Lissorgues, Frédérique Deshours, Christophe Bourcier, Gérard Carrer, Elodie Richalot, Odile Picon

60 GHz square open-loop resonator (SOLR) based on planar Goubau line (PGL) technology

Emad Elrifai[1] ✉, Marjorie Grzeskowiak[1], Gaëlle Lissorgues[2], Frédérique Deshours[3], Christophe Bourcier[1], Gérard Carrer[1], Elodie Richalot[1], Odile Picon[1]

[1]*Université Paris-Est, ESYCOM (EA 2552), UPEMLV, ESIEE-Paris, CNAM, F-77454 Marne-la-Vallée, France*

[2]*Université Paris-Est, ESYCOM (EA 2552), UPEMLV, ESIEE-Paris, CNAM, F-93162 Noisy-le-Grand, France*

[3]*Sorbonne Universités, UPMC Univ Paris 06, UR2, L2E, F-75005, Paris, France*

✉ *E-mail: emadelrifai@gmail.com*

Abstract: This study presents the design, fabrication, and measurement of a square open-loop resonator (SOLR) on high resistivity silicon substrate feed with a planar Goubau line (PGL), which is a very low-loss transmission line around 60 GHz fabricated through a very simple and low-cost process. Electromagnetic simulations using ANSYS high frequency structure simulator are performed for the PGL structure, in order to determine the PGL characteristics (impedance, losses and quality factor) versus the line width. The geometrical parameters of the SOLR structure are studied to observe their impact on reflection and transmission properties. An equivalent lumped element circuit is extracted from the distributed planar design to study and optimise the resonating structure using Advanced Design System. This electrical circuit response is successfully compared to the planar electromagnetic structure one, and a parametric study permits to better understand the role of the different circuit elements. Field displays lead to a better understanding of the SOLR behaviour. For measurement purpose of the fabricated structure, a coplanar waveguide-PGL transition is optimised with 0.9 dB losses. Simulation and measurement results show good performances for filter applications with 1 dB losses and small size at 60 GHz for 10% bandwidth.

1 Introduction

The available unlicensed 7 GHz frequency band between 57 and 64 GHz is dedicated to high data-rate applications, as well as a high level of communication security due to rapid atmospheric propagation attenuation, push device development and research activities at millimetre frequencies.

Among different technologies of transmission lines for 60 GHz circuits [1, 2] the planar Goubau line (PGL) presents the lowest signal attenuation on the millimetre-wave band with an insertion loss (IL) <0.07 dB/mm at 60 GHz on high-resistivity silicon [3]. Moreover, the simplicity of its fabrication process is an advantage as it consists of a single metallic line on a substrate without any ground plane.

The studies on PGL can be categorised into two groups depending on the targeted frequency band, namely the GHz domain between 40 and 70 GHz [4, 5], and the THz domain up to 0.3 THz [6]. In our case, we focus on the millimetre band and the objectives are twofold: using the PGL technology at 60 GHz to design a block that can be one element to build a filter and extract a model with equivalent lumped elements by extraction. Half-wavelength resonators are widely used for filtering applications. As planar band-pass filters are widespread functions in a microwave integrated circuit, several half-wavelength planar resonators were proposed with different transmission line technologies for planar band-pass filters at 60 GHz. Based on the micro-strip lines, the filter in [7] presents an IL <−4 dB at 60 GHz for a bandwidth of 5%.

The use of special materials such as low temperature co-fired ceramics (LTCC) has led to an IL around −3.7 dB with a bandwidth of 3.4% using a coupled-resonator filter [8].

The SOLR was presented earlier with micro-strip technology for planar microwave filters at 2.46 GHz [9]. In this study, we propose a simple two-pole SOLR for filter applications in the millimetre-wave band (57–64 GHz) using PGL technology. First, the feed line (PGL) structure is described, and its characteristic parameters such as impedance and quality factor Q are given. Then the parametric study of the resonator behaviour is performed through electromagnetic simulations using ANSYS high frequency structure simulator (HFSS) software. Besides, an equivalent lumped element circuit is proposed to optimise the resonator response. In order to measure the fabricated SOLR with coplanar probes, we need a coplanar waveguide (CPW)–PGL transition, a simple design CPW-planar Goubau type was first studied for THz BioMEMS application [10, 11], this design was also presented for millimetre-wave applications in [3]. In this work, we have optimised the design defined in [3] after adding a glass wafer below the filter to reduce the probe station metallic chuck effect on the field distribution. Finally, experimental results are compared with simulated data obtained through electromagnetic modelling as well as the related equivalent lumped element circuit.

2 PGL structure

The proposed PGL structure (Fig. 1*a*) consists of a 1 μm thick gold conductor line ($\sigma = 4.1 \times 107$ S/m) deposited on a bi-layer substrate: 350 μm high resistivity silicon substrate ($\varepsilon = 11.6$, $\sigma = 0.025$ S/m) on a 500 μm glass substrate ($\varepsilon = 11.6$, $\tan\delta < 0.001$); the glass substrate has been added to keep away the effect of the metallic surface of the measurement bench. Fig. 1*b* shows the electrical field distribution of the 50 μm width PGL, which is clearly confined near the metallic wire.

The PGL acts as a high-pass filter; substrate's permittivity and thickness have been essentially modified in [3] to reduce the cut-off frequency. The PGL characteristic parameters (characteristic impedance Z_C, attenuation coefficient α, and quality factor QL) are extracted from electromagnetic simulations using HFSS by applying a parametric study to the gold conductor width.

Fig. 2*a* shows an impedance varying at 60 GHz from 100 to 40 Ω for PGL width varying from 50 to 500 μm. Very low attenuation coefficients α between 0.05 and 0.08 dB/mm along with a very high-quality factor defined as $\mathrm{QL} = \beta/(2 \times \alpha)$ (with β the phase constant) and of values between 185 and 300 are obtained for the same width variation (Figs. 2*b* and *c*).

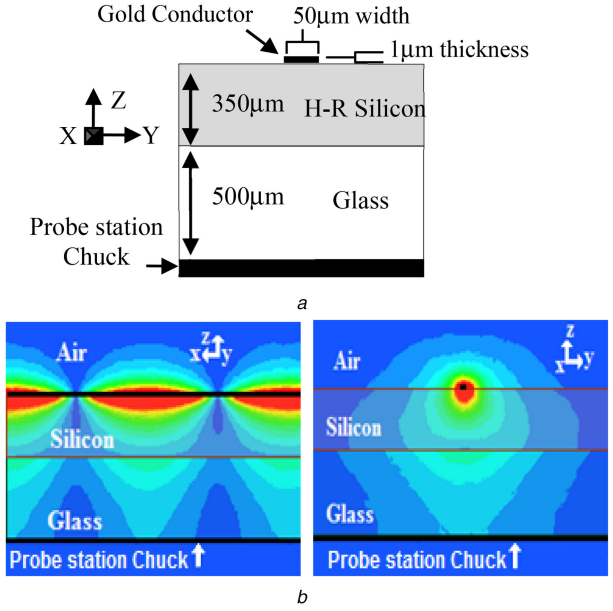

Fig. 1 *Planar Goubau line (PGL)*
(a) PGL over a bi-layer substrate HRS-glass, ***(b)*** E-field magnitude at 60 GHz of the propagating mode in PGL in *xOy* and *yOz* planes (HFSS simulation)

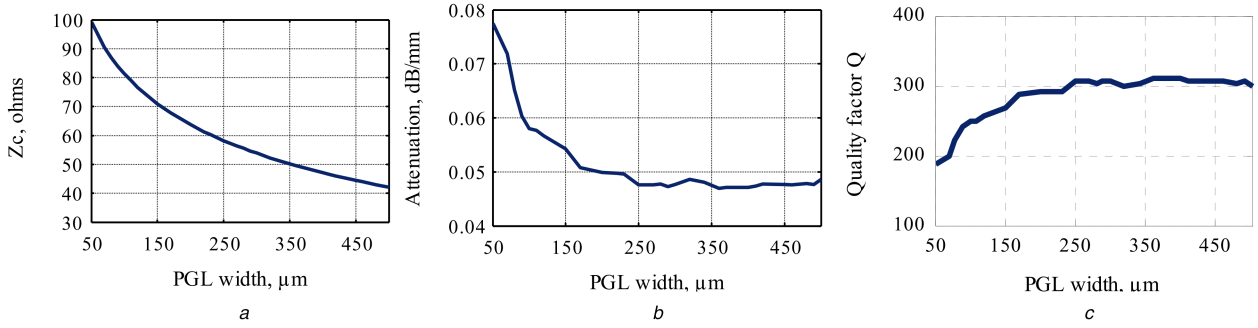

Fig. 2 *PGL characteristic parameters variation at 60 GHz versus strip width*
(a) Characteristic impedance Z_C (Ohm), ***(b)*** Propagation attenuation (dB/mm), ***(c)*** Quality factor

Coupled PGL structure	Coupled PGL width, µm	S_{21} dB
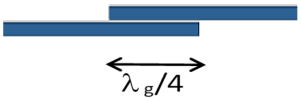	50	-1.9
	100	-2.3
	350	-7.1

Fig. 3 *Comparison of simulated transmission coefficients versus coupled PGL width for a fixed spacing of 10 µm*

3 Square open-loop resonator (SOLR) design

The SOLR will be excited by coupling with a PGL. According to Hong and Lancaster [12], a strong coupling between two microstrip lines can be guaranteed by a small gap between narrow lines.

This coupling condition has been checked with PGLs by simulating the transmission between two coupled PGLs. The total length of both PGLs is 3.75 mm and they are coupled along $\lambda_g/4 = 0.5$ mm (λ_g: PGL guided wavelength), with a spacing between them of 10 µm (that corresponds to our current technological limit). The simulated transmission coefficient is given in Fig. 3. We observe that the use of a narrow PGL permits to strengthen the coupling between the lines: the 50 µm width PGL allows enhancing the transmission between coupled lines up to 1.9 dB. This narrower line presents a characteristic impedance Z_C of 98 Ω and a very low attenuation α below 0.08 dB/mm; it also shows a high-quality factor at 60 GHz $Q = 185$ compared with quality factors obtained with other technologies in the millimetre frequency range: $Q = 34$ in [1], Q up to 40 in [2] and $Q = 16$ in [13]. Fig. 4*a* presents the geometry of the proposed resonator. It consists of two metallic SOLR, each one placed at a distance $d =$ 10 µm from the 50 µm wide central PGL ($Z_C = 98$ Ω) with the following parameters: $W = 50$ µm, $l = 285$ µm, $L = 1.12$ mm $\simeq \lambda_g/2$ at 60 GHz. We defined $r = 20$ µm, $l_c = 285$ µm and $d = 10$ µm. Fig. 4*b* presents the simulation results of the two-pole SOLR, where the S parameters show behaviour of a low pass filter with 1.3 dB IL and 3 dB cut-off frequency of 63 GHz.

A parametric study of the geometrical parameters (resonator opening r, coupling section l_c and distance d between the resonators and PGL) is presented in Fig. 4*c*. It has to be noticed that, in order to keep the resonator total length L constant, the resonator width l has been adjusted while varying r and l_c values. We observe that the resonator opening r has an influence on the resonance frequency, whereas the variation of coupling section l_c can influence the slope of the transmission coefficient after 60 GHz. As expected we can observe the weakness of the resonator effect with an increased coupling distance d due to the low coupling with the exciting PGL.

In the following study, we have added a gap of distance $C = 20$ µm at the middle of the central PGL (Fig. 5*a*).

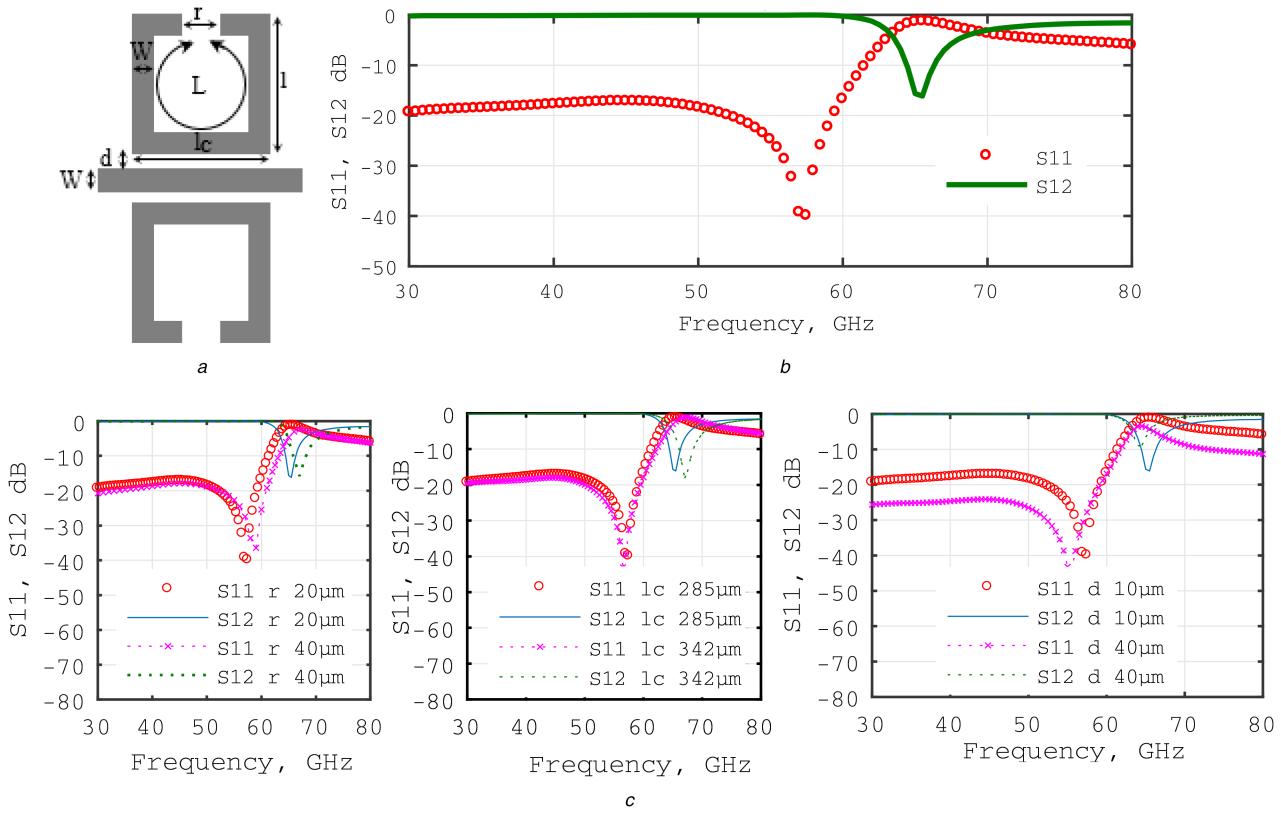

Fig. 4 *SOLR structure with central coupling PGL*

(a) Structure design, ***(b)*** Simulated *S*-parameters of the SOLR structure (reference case), ***(c)*** Variation of the opening *r*, the coupling length l_c and the line spacing *d*

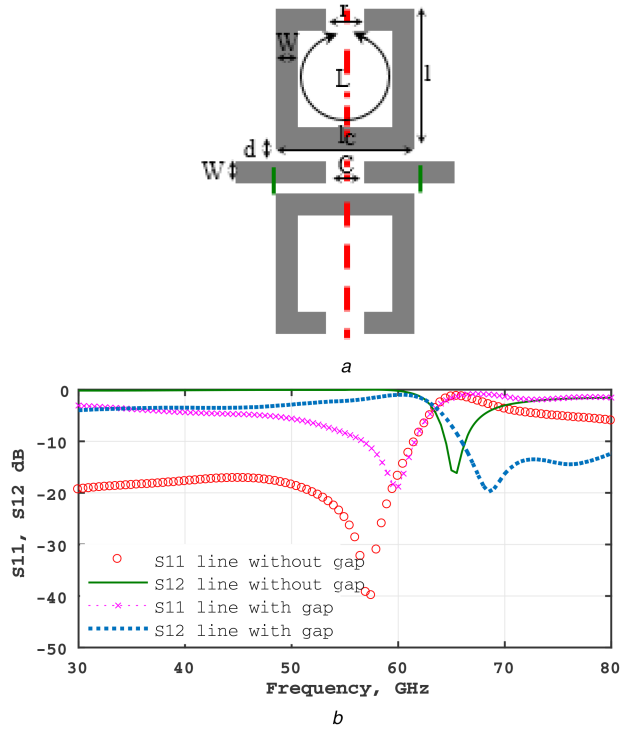

Fig. 5 *SOLR structure with a gap at the middle of the central PGL*

(a) Structure design, ***(b)*** Comparison of simulated *S*-parameters of the SOLR structure with and without the gap on the central PGL

The simulation of the new design shows a drop in the transmission at low frequencies, leading to a large bandpass filter behaviour between 43 and 63.5 GHz (corresponding to a transmission 3 dB below the maximal one) with a maximal transmission coefficient of −0.95 dB at Fc = 60.5 GHz (Fig. 5*b*).

To better understand the influence of the different system elements, we propose an equivalent electrical circuit of the new structure with a gap (Fig. 6*a*), where both coupled SOLRs are modelled as equivalent inductance Lr and capacitance Cr in parallel forming a resonant circuit coupled to the transmission line with a mutual inductance *M*. This circuit can be simplified as a resonant circuit in series with the transmission line composed of the inductance Lr″ and the capacitance Cr″, which are functions of the inductance Lr, the capacitance Cr and the mutual inductance *M* [14].

Lumped element values are determined at 60 GHz through HFSS simulations. To extract the inductance *L* representing the line and the capacitance Cg representing the small discontinuous PGL section from electromagnetic simulations, we firstly consider the continuous PGL leading to the *L* value, then the discontinuous PGL is simulated and the de-embedding of the line accesses permits to extract the capacitance Cg equivalent to the gap [12]. The values of Cr and Cg capacitances are equal to the dimensions of these openings are the same. Lr is then extracted from the resonance frequency of both coupled SOLRs, without considering the excitation line effect. Finally, the coupling coefficient is obtained by fitting the global equivalent circuit response with HFSS results.

The comparison of *S*-parameters simulation results of the lumped element equivalent circuit using Advanced Design System (ADS) software and of the planar filter structure using HFSS tools shows a good agreement between electrical and electromagnetic simulations (Fig. 6*b*) from 50 to 70 GHz. Discrepancies were expected at very lower or larger frequencies than the one where the equivalent lumped element have been determined.

The obtained equivalent circuit is well suited to parametric studies. Fig. 7*a* presents the *S* parameters simulation of the initial lumped element electrical circuit (Fig. 6*a*); the maximal transmission and minimal reflection coefficients are obtained at Fc = 60 GHz, and a 17.5 GHz bandwidth is obtained between 47 and 64.5 GHz (corresponding to transmission coefficients 3 dB below its maximal value).

Fig. 7*b* shows the influence of Cg capacitance value. Its decrease of 20% leads to an Fc increase of 2 GHz associated with a narrower bandwidth of 11 GHz between 53.5 and 64.5 GHz. Reversely, the +20% variation of capacitance Cg induced an Fc decrease of 3.33% down to 58 GHz with a larger bandwidth of 22 GHz between 42 and 64 GHz (Fig. 7*b*). The −20% variation of the

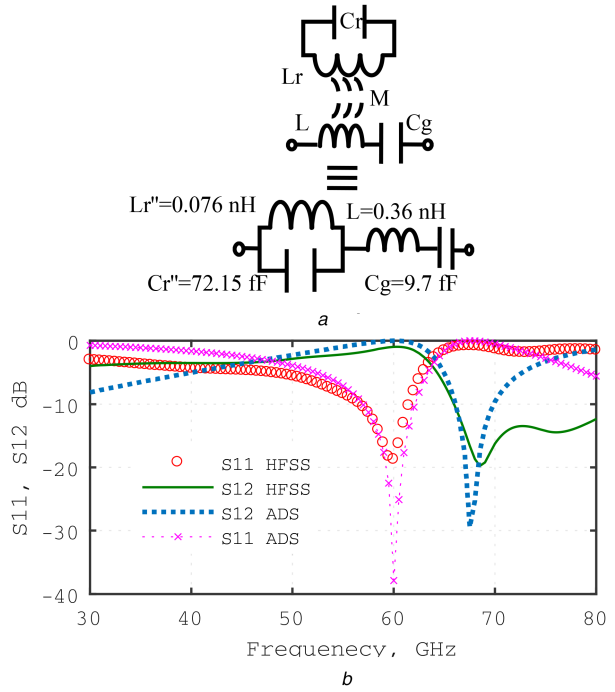

Fig. 6 *Equivalent circuit*

(a) Lumped element equivalent circuit, ***(b)*** Comparison of *S*-parameters for lumped elements ADS & electromagnetic HFSS simulations

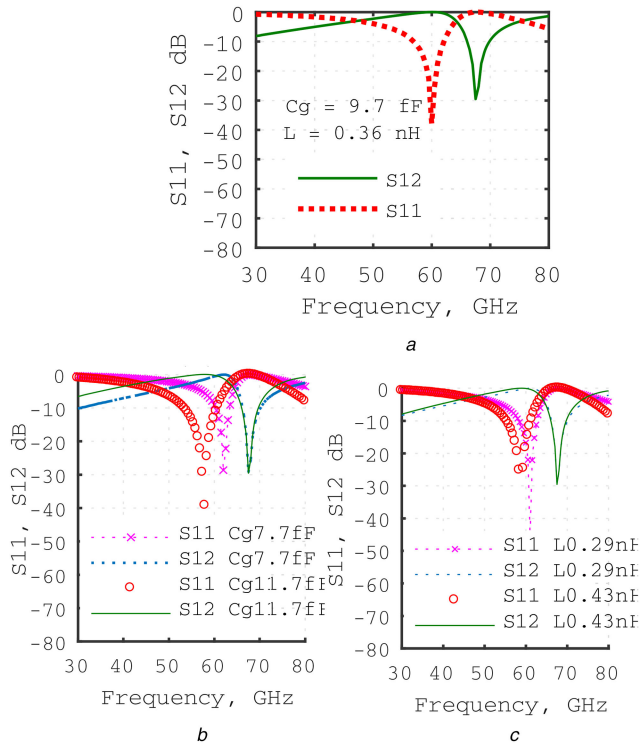

Fig. 7 *Electrical circuit study*

(a) ADS simulation of the initial electrical circuit (Fig. 6*a*), ***(b)*** Variation ±20% of capacitance Cg representing the central line gap, ***(c)*** Variation ±20% of inductance *L* representing the PGL line

inductance *L* results in a +2.5% frequency shift for Fc to 61.5 GHz with a bandwidth of 15 GHz between 49 and 64.5 GHz, while the +20% variation of inductance *L* leads to a −1.66% frequency shift for Fc to 59 GHz with a bandwidth of 19.5 GHz between 45.5 and 64 GHz (Fig. 7*c*). Therefore, we can conclude that the resonance frequency and transmission bandwidth are more sensitive to Cg than to other parameters.

The *E* and *H* field cartographies for the reference structure (Fig. 5*a*) have been observed at different frequencies to understand the variation trend of magnetic coupling versus the operation frequency.

Magnetic coupling occurs between the central line and the two SOLR, as well as between the two SOLRs. Fig. 8*a* shows magnetic lines at three frequencies and that the magnetic coupling is higher at 60 GHz (minimal reflection) than at other frequencies (50, 70 GHz). The attenuation of the electric field through the SOLR (Fig. 8*b*) is clearly seen at 70 GHz while it seems less efficient at 50 GHz in comparison with 60 GHz where the higher transmission is concomitant with high excitation of both resonators; this illustrates the SOLR behaviour.

4 Measurements

The reference structure (Fig. 5*a*) was measured on the wafer using 150 µm pitch ground-signal-ground (GSG) probes and a vectorial network analyser operating up to 67 GHz [15]. A line reflect match calibration technique is used to eliminate systematic measurement errors due to the imperfections of the analyser and test setup. In order to measure the performances of the SOLR, we add a CPW–PGL transition between the coplanar measurement accesses (suited for 150 µm pitch probes in GSG configuration) and the PGL of 50 µm width.

The strip width remains constant at 50 µm along the whole transition. To have a 50 Ω characteristic impedance at the CPW access, the transition begins with a 250 µm long CPW Fig. 9*a* Section I, with slots of width s fixed to 30 µm. It continues with an elliptical taper of 1.5 mm length (Fig. 9*a* section II).

Fig. 9*b* presents the display of electric field amplitude along the CPW–PGL transition, where we observe its gradual decrease on both ground planes of elliptical shape from the CPW line to the Goubau line. Fig. 9*c* presents the field distribution on transition cross-sections situated at the beginning and the end of the transition; it shows the coplanar mode (with electric field arrows pointing from the central line to the ground planes) turns into a PGL mode (with electric field lines distributed radially around the line strip). Fig. 9*d* presents the transition *S* parameters obtained through simulations and measurements. Very good performances better than [3] are obtained for this transition with a reflection coefficient below −14 dB and a transmission coefficient above −1.8 dB on the whole frequency band: the transition's losses in [3] were elevated and mask transmission lines with low losses. In [3], a very long transmission line, i.e. with a length corresponding to 10 times the guided wavelength, was used to extract the line's losses. In the previous study, the experimental transition has to be improved, which has been done in this present study: the structure's length was less than four times the guided wavelength. The loss data is equal to 1.78 dB for back-to-back CPW–PGL–CPW transitions, and to 0.89 dB for a single CPW–PGL transition. We report size, resonant frequency, bandwidth and losses for different transitions in Table 1. This value is of the same order of the state-of-the-art with smaller size and selective frequency band. The line losses can be correctly obtained with this transition.

In order to extract the response of the measured SOLR structure with discontinuities (Fig. 5*a*) from the raw measurements (Fig. 10*a*; to remove the transition influence), several devices are inserted between both transitions, namely a null-length line, a line of non-null length, and an open circuit, according to the through, reflect, line (TRL) extraction technique [18]. The measurement of these devices also permits the extraction of the *S*-parameters of the transition as presented in Fig. 9*b*.

Fig. 10*b* compares the simulated and measured SOLR after transition de-embedding, showing a good agreement between simulation and measurement, with a very low IL <1 dB at 60 GHz, and a return loss <−10 dB between 58 and 61 GHz. Fig. 10*c* compares measured transmission and reflection coefficients with those obtained with ADS lumped element modelling; it shows the lumped element equivalent circuit correctly represented the resonator behaviour until 67 GHz.

The quality factor of a band-pass filter is defined as the ratio of the centre frequency to the frequency bandwidth (FBW). This gives a measure of the pass-band and can be used to describe the filter selectivity. The measurement of the proposed SOLR leads to

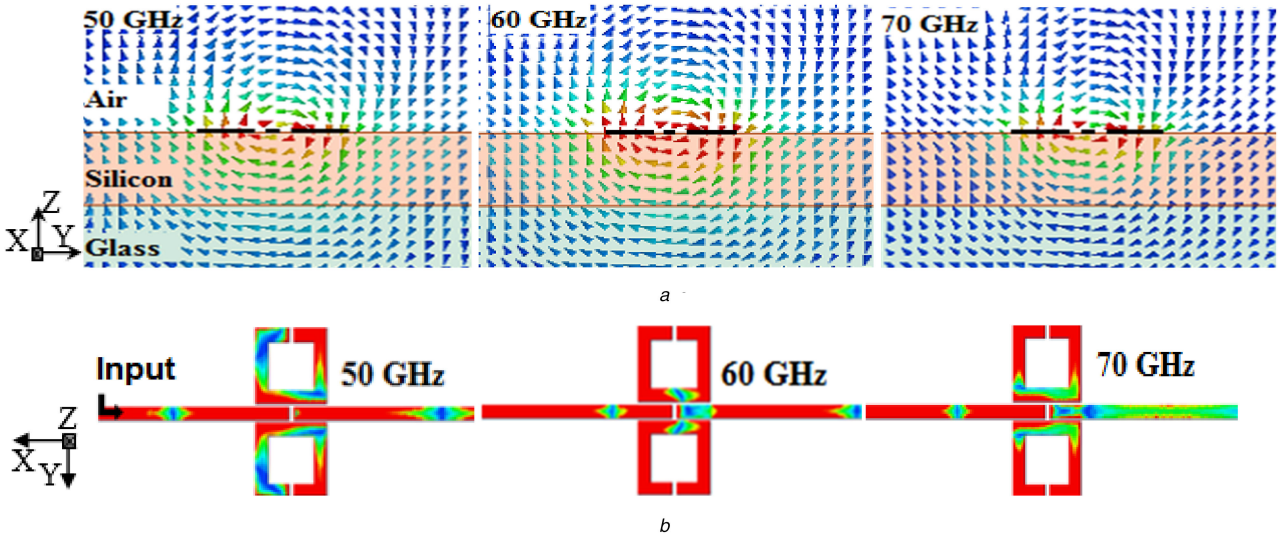

Fig. 8 *Electromagnetic cartographies*

(a) Cross-section plane for magnetic field lines at the centre of the SOLR (red dashed line Fig. 5*a*) at three frequencies (50, 60, 70 GHz), with the same colour scale, ***(b)*** Electric field amplitude on the metallisation at three frequencies (50, 60, 70 GHz), with the same colour scale

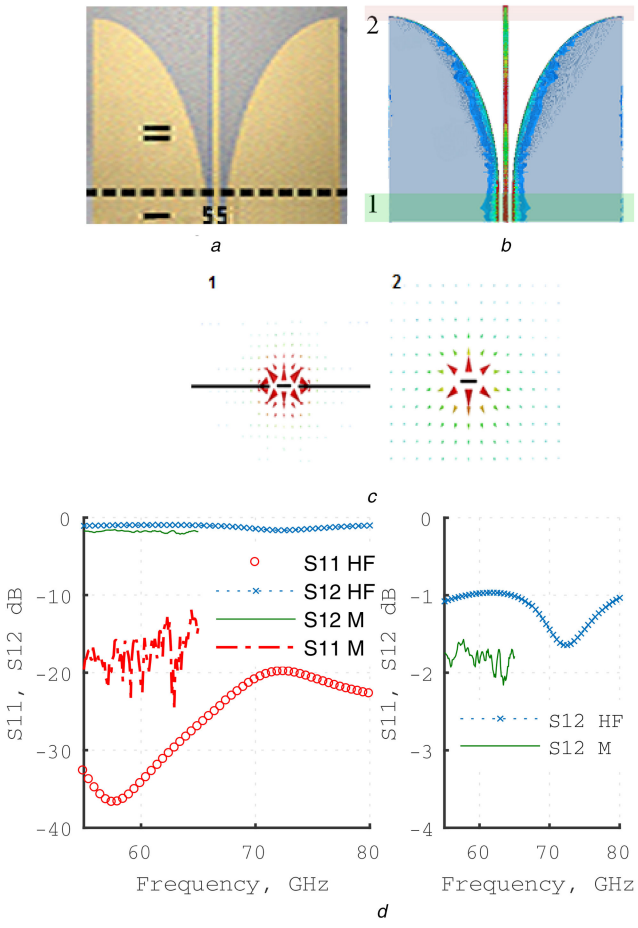

Fig. 9 *CPW–PGL transition*

(a) Fabricated CPW–PGL transition, ***(b)*** Electric field display along CPW–PGL transition at 60 GHz, ***(c)*** Electric propagation modes: one CPW area, two PGL area, ***(d)*** Transmission and reflection coefficients (S11, S12) from de-embedded measurement (*M*) and HFSS

a quality factor Q_F of 9.5 (FBW of 6.5 GHz between 56 and 62.5 GHz) with 1 dB IL at 60 GHz, which is comparable to [19] with quality factor $Q_F = 11.62$ and 2.26 dB IL at 60 GHz. When we compare with [19], the measured quality factor is of the same order, but with a technological process easier (only one metallisation), and smaller size (0.64 mm × 0.285 mm for the PGL structure and 6.2 mm × 3.7 mm for [19]). Further comparisons with millimetre-band band-pass filters presented in the literature are given in Table 2. They show this studied filter presents very promising properties for 60 GHz filtering applications.

5 Conclusion

Besides the very simple related technological process, as their fabrication only requires a single metal deposition, PGL benefits from very low losses in the millimetre frequency band; according to electromagnetic simulation, their transmission losses are <0.07 dB/mm with a very high-quality factor >175. Therefore, PGL technology with one single metallisation on silicon has been proposed used to obtain millimetre components, such as transmission line and resonator. As a CPW access is necessary to characterise the obtained structure using a probe station, a CPW–PGL–CPW transition was optimised between 57 and 64 GHz, with a reflection coefficient <−14 dB and a transmission coefficient above −1.8 dB on the whole frequency band

This paper focused on a half wavelength SOLR coupled to a PGL. Measurement results confirmed by electromagnetic simulations using HFSS software show we obtain a pass-band filter of FBW 6.5 GHz between 56 and 62.5 GHz with 1 dB IL at 60 GHz. Electric and magnetic field displays show the gradual transformation of the propagation mode from CPW mode to PGL one along the optimised transition and highlight the coupling between both resonators at the resonance frequency. An equivalent electrical model extracted from distributed electromagnetic design has been used for parametric studies on the circuit elements using ADS software. The agreement between the electromagnetic simulation using HFSS and ADS simulation of the proposed lumped element equivalent circuit opens the door to optimisation of the resonator response for future band-pass filter application as well as the integration of the SOLR structure to more complex devices. The good transmission properties with very low losses and the good agreement between measurement and simulation results encourage further developments of higher order filters (four-pole and six-pole SOLR) based on the proposed resonant cell to improve the filter response at a low frequency band, also for other studies on coupled line filters.

Further studies aimed to deeper understand the behaviour of this resonating structure and allow its adaptation to a specific application. In our study, we focus on a half wave length resonator that can be seen as one block. The characteristic of a filter can be performed by using several blocks and adjusting the characteristics of each block to response to the filter specifications for instance: we can control the behaviour of each resonator by adding or removing some elements or by changing the interaction between the blocks.

Table 1 Comparison of fabricated transitions in state-of-the-art

Ref	Type	Size, mm	f_0, GHz	Bandwidth (BW), %	Single transition less than
[16]	coplanar to microstrip waveguide	Ø	60	7	1.7 dB
[17]	substrate-integrated image guide to conductor-backed CPW	Ø	62	17.7	0.748 dB
our work	coplanar to Goubau line	$1.75 \times 0.90.35 \times 0.18\ \lambda_0^2$	60	5	0.9 dB

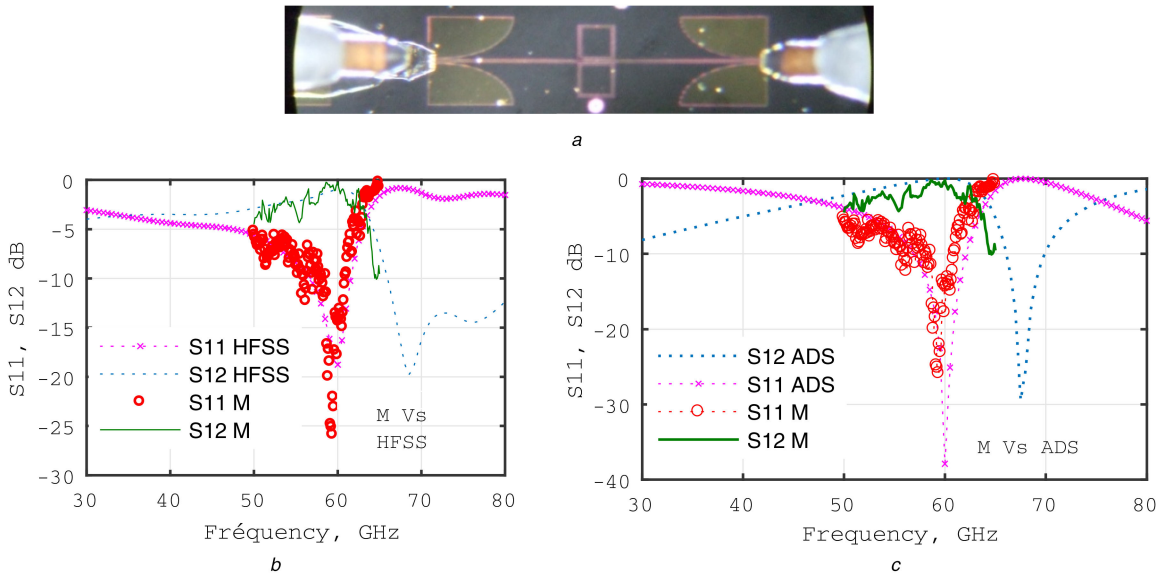

Fig. 10 *Measurement of the SOLR*

(a) Filter under measurement with coplanar probes, ***(b)*** S21 and S11, electromagnetic simulation with HFSS and de-embedded measurements (*M*), ***(c)*** S21 and S11, lumped elements simulation of equivalent circuit (Fig. 4*b*) with ADS (ADS) and de-embedded measurements (*M*)

Table 2 Comparison of 60 GHz band-pass resonator filters

Ref	f_0, GHz	BW, %	IL at 60 GHz, dB	Return loss, dB	Technology	Area
[7]	60	5	<4	>17	micro-strip	<1 mm^2
[8]	61	3.4	3.7	>10	LTCC	1.274 mm^2
[19]	60	4.5	4.9	21	LTCC	2.36^2 × 1.1 mm^3
our SOLR	60	10.1	1	>10	PGL	<1 mm^2

6 References

[1] Tang, X.L., Franc, A.L., Pistono, E., *et al.*: 'Performance improvement versus CPW and loss distribution analysis of slow-wave CPW in 65 nm HR-SOI CMOS technology', *IEEE Trans. Electron Devices*, 2012, **59**, (5), pp. 1279–1285, doi: 10.1109/TED.2012.2186969

[2] Serrano, A.L.C., Franc, A.-L., Assis, D.P., *et al.*: 'Slow-wave microstrip line on nanowire-based alumina membrane'. 2014 IEEE MTT-S Int. Microwave Symp. (IMS), Tampa, FL, 1–6 June 2014, pp. 1–4, doi: 10.1109/MWSYM.2014.6848552

[3] Emond, J., Grzeskowiak, M., Lissorgues, G., *et al.*: 'Low loss Goubau line on high-resistivity silicon in the 57–64 GHz band'. Proc. 5th European Conf. on Antennas and Propagation (EUCAP), 2011, pp. 1459–1462

[4] Xu, Y., Nerguizian, C., Bosisio, R.G.: 'Wideband planar Goubau line integrated circuit components at millimetre waves', *IET Microw. Antennas Propag.*, 2011, **5**, (8), pp. 882–885

[5] Xu, Y., Bosisio, R.G.: 'Wideband planar Goubau line (PGL) couplers and six-port circuits compatible with short range (60 GHz) radio', *IET Microw. Antennas Propag.*, 2013, **7**, (12), pp. 985–990

[6] Zehar, M., Moreno, G., Chahadih, A., *et al.*: 'Low loss terahertz planar Goubau line on high resistivity silicon substrate'. 13th Mediterranean Microwave Symp. (MMS) Conf., Saida, Lebanaon, 2–5 September 2013, pp. 1–3, doi: 10.1109/MMS.2013.6663115

[7] Amano, Y., Yamada, A., Suematsu, E., *et al.*: 'Low cost planar filter for 60 GHz applications'. 30th European Microwave Conf., Paris, France, October 2000, pp. 1–4, doi: 10.1109/EUMA.2000.338630

[8] Amaya, R.E.: 'A layout efficient, vertically stacked, resonator-coupled bandpass filter in LTCC for 60 GHz SOP transceivers'. 2010 IEEE Radio Frequency Integrated Circuits Symp. (RFIC), Anaheim, CA, 23–25 May 2010, pp. 245–248, doi: 10.1109/RFIC.2010.5477319

[9] Hong, J.-S., Lancaster, M.J.: 'Couplings of microstrip square open-loop resonators for cross-coupled planar microwave filters', *IEEE Trans.*, 1996, **MTT-44**, pp. 2099–2109

[10] Akalin, T., Treizebré, A., Bocquet, B.: 'Single-wire transmission lines at terahertz frequencies', *IEEE Trans. Microw. Theory Tech.*, 2006, **54**, (6), pp. 2762–2767

[11] Treizebré, A., Akalin, T., Bocquet, B.: 'Planar excitation of Goubau transmission lines for THz BioMEMS', *IEEE Microw. Wirel. Compon. Lett.*, 2005, **15**, (12), pp. 886–888

[12] Hong, J.-S.G., Lancaster, M.J.: '*Microstrip filters for RF/microwave applications*', vol. **167** (John Wiley & Sons, Hoboken, NJ, USA, 2004)

[13] Mat, D.A.A., Pokharel, R.K., Sapawi, R., *et al.*: 'Low-loss 60 GHz patterned ground shield CPW transmission line'. TENCON 2011-2011 IEEE Region 10 Conf., 2011, pp. 1118–1121

[14] Martín, F., Bonache, J., Falcone, F., *et al.*: 'Split ring resonator-based left-handed coplanar waveguide', *Appl. Phys. Lett.*, 2003, **83**, (22), pp. 4652–4654, doi: 10.1063/1.1631392

[15] Keysight Technologies. Available at http://www.keysight.com

[16] Zandieh, A., Ranjkesh, N., Safavi-Naeini, S., *et al.*: 'A low-loss CPW to dielectric waveguide transition for millimeter-wave hybrid integration'. IEEE Antennas and Propagation Society Int. Symp. (APSURSI), July 2012

[17] Cheng, Y.J., Bao, X.Y., Guo, Y.X.: 'LTCC-based substrate integrated image guide and its transition to conductor-backed coplanar waveguide', *IEEE Microw. Wirel. Compon. Lett.*, 2013, **23**, (9), pp. 450–452

[18] Rubin, D.: '*De-embedding millimeter-wave integrated circuits with TRL*' (Naval Ocean Systems Center, San Diego, CA, 1991)

[19] Wang, D., Chin, K-S., Che, W., *et al.*: 'Compact 60 GHz low-temperature cofired ceramic filter with quasi-elliptic bandpass response', *IET Microw. Antennas Propag.*, 2016, **10**, (6), pp. 664–669